Doi: 10.31276/VJSTE.61(2).23-28

Synthesis and application of graphene aerogel as an adsorbent for water treatment

Thi Lan Nguyen[1], Tri Tin Nguyen[1], Hoang Tu Tran[1], Minh Dat Nguyen[1], Huu Hieu Nguyen[1, 2*]

[1]Key Laboratory of Chemical Engineering and Petroleum Processing
[2]Faculty of Chemical Engineering
University of Technology - Vietnam National University, Ho Chi Minh city

Received 1 June 2018; accepted 1 August 2018

Abstract:

In this research, graphene aerogel (GA) was fabricated by chemical reduction method, in which ethylenediamine (EDA) was used as a reducing and functionalising agent. The characterisation of GA was studied by density, field-emission scanning electron microscope, Brunauer-Emmett-Teller (BET) specific surface area, Fourier transform infrared spectroscopy, and X-ray diffraction. The results of the analysis showed that GA exhibits low density, ranging from 4-8 mg/cm^3, high porosity, and BET specific surface area changes from 176 to 1845 m^2/g. It was found that the suitable content of EDA on the synthesis of GA is 30 µl. The obtained GA was used as an adsorbent for removal of oils and methylene blue (MB) from aqueous solutions. The maximum adsorption capacities of GA for lubricant and crude oils are 160 g/g and 110 g/g respectively. The effecting factors including pH, contact time, and initial concentrations on the adsorption capacity of GA for MB were investigated. The adsorption process of MB onto GA followed the *pseudo-second-order* kinetic and well-fitted to Langmuir isotherm model. The maximum adsorption capacity for MB from linear Langmuir model was calculated to be 212.76 mg/g at pH 7. Accordingly, GA could be used as a potential adsorbent for removal of oils and MB from water.

Keywords: **chemical reduction, crude oil, graphene aerogel, lubricant oil, methylene blue.**

Classification number: **2.2.**

Introduction

Water, an important resource in nature, has significant impacts on the living conditions of creatures on the earth. However, rapid industrialisation and urbanisation have resulted in water pollution. The pollutants, such as metal ions, oils, organic dyes, etc., are released into the environment, which cause serious problems for the environment, humans, and other organisms. Many methods have been developed, such as adsorption, chemical oxidation, electrochemical, biological, membrane separation, ion exchange, etc. for removal of toxic contaminants from water. Adsorption is one of widely used procedure for removal of pollution from water. The traditional absorbent materials showed low adsorption capacity and faced difficulty in separating pollutants like activated carbon, zeolite, natural clays, agricultural waste, biomass, polymeric, etc. [1, 2].

Recently, graphene (Ge), a single atomic layer graphite, has attracted great interest among scientists. Ge has unique properties such as chemical stability, excellent mechanical strength, high electrical and thermal conductivities and good optical and large specific surface area. Ge is used in many applications including catalyst, energy-storage and environmental. However, Ge nanosheets tend to aggregate and restack, leading to significant reduction of specific surface area and application ability [3, 4]. To solve this problem, three-dimensional (3D) graphene nanomaterials, especially graphene aerogel (GA), are being developed. GA has unique features like low weight, high porosity, large surface area and chemical stabilities. Based on these properties, GA materials have been considered as ideal adsorbents for water treatment.

Several methods have been applied to synthesise GA including 3D printing, cross-linking, hydrothermal reduction, organic functionality and template-directing method. However, these methods are difficult to control in synthesis conditions, the research process of 3D-

*Corresponding author: Email: nhhieubk@hcmut.edu.vn

GA is limited [5-8]. In recent years, chemical reduction method has developed benefits like simple, environmental friendly, reduction at low temperature (T<100^{0}C), and easy scalability, which is why it is commonly used to synthesise GA. The mild reduction agents such as acid ascorbic, sodium ascorbate, ammoniac, urea, ethylenediamine (EDA), etc. are widely used to synthesise GA. During the reduction process, Graphene oxide (GO) was changed to reduced graphene oxide (rGO) nanosheets, the electrostatic repulsion was decreased. As a result the performance of self-assembly of rGO was enhanced to form network structure [9, 10].

In this study, GA was synthesised by chemical reduction method using EDA as a reducing agent. Effect of EDA content on the synthesis of GA was studied. The structure and morphology of GA were characterised by calculating apparent density, field-emission scanning electron microscope (SEM), Brunauer-Emmett-Teller (BET) specific surface area, Fourier transform infrared spectroscopy (FTIR), and X-ray diffraction (XRD). The obtained GA was used as an adsorbent for removal of oils and methylene blue (MB) from water.

Materials and methods

Materials

Graphite powder with an average particle size of 20 µm and EDA solution (99%) was purchased from Sigma Aldrich, Germany. Potassium permanganate (99%), ethanol (99%) and hydrogen peroxide (30%) were obtained from VN Chemsol, Vietnam. Sulfuric acid (98%), phosphoric acid (85%), hydrochloric acid (36%) and MB (99%) were purchased from Xilong Chemical, China. Lubricant and crude oils were supplied from Petrolimex, Vietnam. Twice-distilled water was used in all experiments.

Synthesis of GA

GO was synthesised using the improved Hummers method as mentioned in our previous work [11]. In a typical process, GO was dispersed into water with concentration of 5 mg/ml. Then, different content of EDA was added to GO suspension. The mixture was heated at 90^{0}C for 6 hours to form graphene hydrogel (GH). Then, GH was immersed and exchanged in ethanol and deionized water for at least 5 times to remove extra EDA and other impurities. Finally, GH was sublimated at -60^{0}C for 48 hours to obtain GA. The sample with EDA content of 15, 30, 45 and 60 µl are labelled as GA15, GA30, GA45 and GA60.

Characterisation

The dimension of GA was measured by a caliper (VOREL-15240, Germany) to calculate the volume. The weight was determined by analytical balance (Sartoius CPA225D, Germany). The density of GA is its mass per unit volume, which was calculated using the following equation:

$$p = \frac{m}{V} \quad (1)$$

where p is the density (mg/cm^3), V is the volume (cm^3) and m is weight (mg) of GA.

The morphology of samples was studied using the FE-SEM images (S-4800, Hitachi, Japan). The surface area and pore volume of GA were determined by BET method with a Nova 1200e instrument (Quantachrome, USA). The void-space of GA was calculated from pore volume results. The porosity is a ratio of the void-space and bulk volume of material, which was obtained from equation (2).

$$\varepsilon = \frac{v_V}{v_T} 100\% \quad (2)$$

where Ɛ is the porosity (%); V_v and V_T are the pore volume and the bulk volume of materials (cm^3/g) respectively. FTIR spectra was recorded with an Alpha-E Brucker (Brucker Optik GmbH, Ettlingen, Germany) spectrometer ranging in wavenumber from 500 to 4000 cm^{-1} to study the functional groups on the surface of materials. XRD patterns were performed on an X-ray Diffusion instrument (D8 Advance, Brucker, Germany).

Oil adsorption

The adsorption capacity of GA for oil was determined with the help of the weight method. First, the GA sample was weighed (W_i) then put into crude or lubricant oils. After being fully adsorbed, the sample was taken out. After removing oil residue on the surface with filter papers, the sample was weighted (W_f). The oil adsorption performance was reflected by the saturated adsorption capacity per unit mass of the GA samples, which was showed by the following equation:

$$q_{oil} = \frac{W_f - W_i}{W_i} \quad (3)$$

where q_{oil} is the adsorption capacity for oil at saturated state. W_i and W_f are the initial and final weights (at adsorption saturation) of GA respectively [3, 12].

Methylene blue adsorption

The adsorption experiments were conducted to study adsorption behaviour and kinetics process of dyes adsorption. Batch experiments were performed by adding 20 mg of adsorbent into 20 ml of MB solution with constant shaking (100 rpm) at room temperature to study the effects of contact time (time: 0-1440 min, pH 6, C_o 200 mg/l), pH values (pH 3-10, C_o 200 mg/l, equilibrium time), and initial concentration (C_o 50-400 mg/l, equilibrium time, optimal pH). After adsorption equilibrium, the residual concentration of MB was measured by UV-Vis spectrophotometer (Dual FL, Horiba, Japan) at the wavelength of 664 nm. The adsorption capacity (q) was calculated using the following equation:

$$q = \frac{(C_0 - C_e)\,V}{m} \quad (4)$$

where C_0, C_e are the concentration of MB before and after the adsorption, V is the volume of MB solution (ml) and m is the weight of material (mg).

The *pseudo-first-order* and *pseudo-second-order* models were applied to study the adsorption kinetic. The equation of models are as follows:

$$ln(q_e - q_t) = lnq_e - k_1 t \quad (5)$$

$$\frac{t}{q_t} = \frac{1}{k_2 q_e^2} + \frac{1}{q_e} t \quad (6)$$

where q_e and q_t are the amounts of MB adsorbed on the surface of GA at equilibrium and at time t (mg/g) respectively; k_1 and k_2 are the *pseudo-first-order* and *pseudo-second-order* constant respectively.

In order to evaluate the adsorption capacity of adsorbent, the experiment data was analysed using the Langmuir and Freundlich isotherms models. The linear equation models were presented by the following equations:

$$\frac{C_e}{q_e} = \frac{C_e}{q_m} + \frac{1}{q_m k_l} \quad (7)$$

$$lnq_e = lnk_f + \frac{1}{n} lnC_e \quad (8)$$

where q_m is the maximum uptake capacity (mg/g), C_e is the concentration of MB solution at equilibrium (mg/l), and k_l is the Langmuir constant (l/mg); k_f and n are the Freundlich constants [2, 13].

Results and discussion

Characterisation

Density of GA: the 3D-structure of GH was formed by self-assembling of rGO through hydrogen bonds, π-π interactions, and Van der Waals forces [9, 14]. Then, the freeze drying process was conducted. After sublimation, the content of water in structure was removed but the morphology of GA still remained with very low density ranging from 4 to 8 mg/cm as shown in Table 1.

Table 1. Density of GA.

Sample	GA15	GA30	GA45	GA60
p (mg/cm^3)	6.37	4.57	6.76	7.95

SEM images: the porous structure of GA was studied as shown in Fig. 1. As can be seen, GA was described using a honeycomb-like 3D porous structure with the pore size ranging from 5-80 µm. Among that, the obtained GA30 had optimum pore size of the network, which is the highest, approximate a hundred micrometres. This pointed out that the partial over-lapping of coalescing of rGO nanosheets occurred due to partial restoration of sp^2 regions, π-π stacking, and cross-linking under the effect of EDA, leading to the formation of 3D-architecture [7, 15].

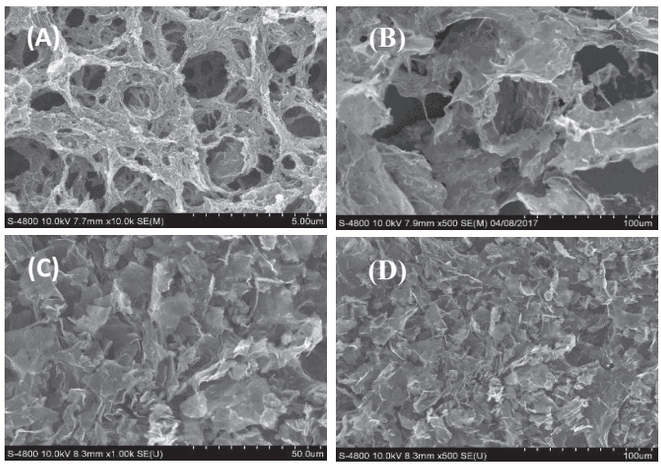

Fig. 1. SEM images of GA15 (A), GA30 (B), GA45 (C), and GA60 (D).

FTIR spectra: Fig. 2 shows the FTIR spectra of GO and GA. The characteristic peaks of GO appear at 1734, 1650, 1229 and 1055 cm^{-1} corresponding to C=O, C=C, C-O, and C-O-C groups respectively [3, 11]. For GO aqueous solution treated with EDA, the characteristic peaks of C=O, C-O groups were decreased, and the new peaks were 1550 and 1190 cm^{-1} relating to the vibration of N-H and C-N groups respectively. These results confirmed that the nucleophilic reaction between the epoxide group in rGO and the amine group in EDA resulted in crosslink between the rGO nanosheets to form porous framework [15, 16].

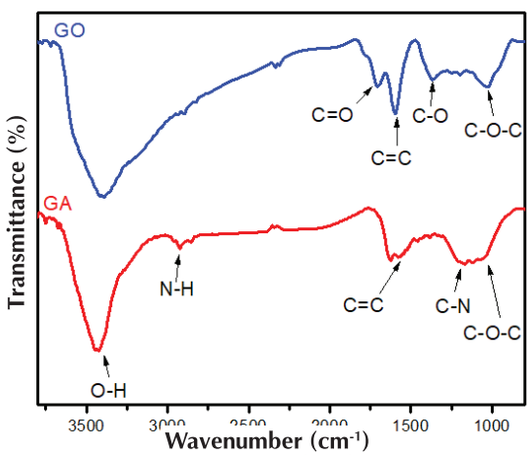

Fig. 2. FTIR spectra of GO and GA.

XRD patterns: the structural phases and interlayer spacing of GO and GA were studied by XRD as shown in Fig. 3. For GO, XRD pattern shows a sharp peak at 2θ = 10.6^0 with an interlayer spacing is 8.32 Å. This result indicated the formation of oxygen-containing groups on the surface of graphene nanosheets. For GA, a wide peak at 2θ = 23.65^0 appeared with an interlayer distance of 3.67 Å. The interlayer distance of GA is larger than that of graphite

(3.4 Å), which explains the fact that the oxygen-containing functional groups on GO surface were partially reduced and rGO self-assembled to form a 3D-architecture [15, 17, 18].

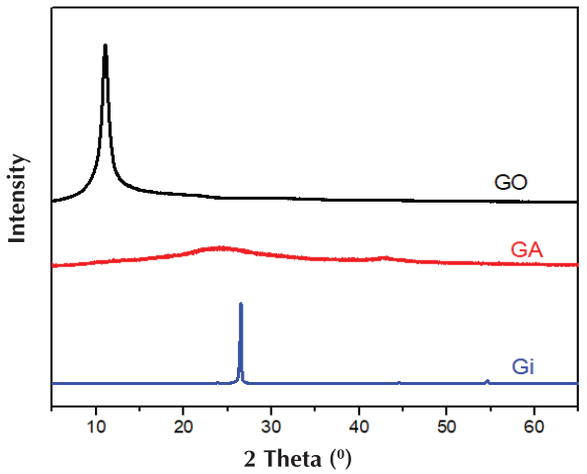

Fig. 3. XRD pattern of Gi, GO, and GA.

BET specific surface area: BET was used to calculate the specific surface area of GA, which is shown in Table 2. This result can be explained by the self-assembly process of rGO nanosheets to form interconnected structure with large pore volume, leading to an increase in the surface area of GA [19]. These BET results were in good agreement estimated from the SEM images. GA30 had the specific surface area of 1845 m^2/g and the porosity of 98.06% was the selected adsorbent for the following experimental adsorption.

Table 2. BET Specific surface area of GA.

Samples	GA15	GA30	GA45	GA60
Specific surface area (m^2/g)	576	1845	285	176

Oil adsorption

Due to their light weight, high porosity structure, large specific surface area and excellent hydrophobicity, GA was used as an absorbent material for oils. The adsorption efficiency of GA for lubricant and crude oils is shown in Table 3.

Table 3. The adsorption capacities of GA for oils.

Sample	GA
Lubricant oil (g/g)	160
Crude oil (g/g)	110

The adsorption capacity of GA for lubricant oil 160 g/g was larger than that for crude oil 110 g/g. The adsorption capacity depends on density of oil and it was found that the adsorption increases as per the density of the materials. The results were in agreement with previous study suggesting that GA has large pores and high surface area, resulting in higher oil adsorption capacity [16].

Effect of conditions on methylene blue adsorption

Contact time: the effect of contact time was carried out at initial concentrations of 200 mg/l as shown in Fig. 4. The adsorption was increased rapidly at 240 mins and the equilibrium was established after 480 mins. This suggests that the network structure of GA with large area and volume pores increased exposure and diffusion rate of MB for adsorption sites on surface of GA.

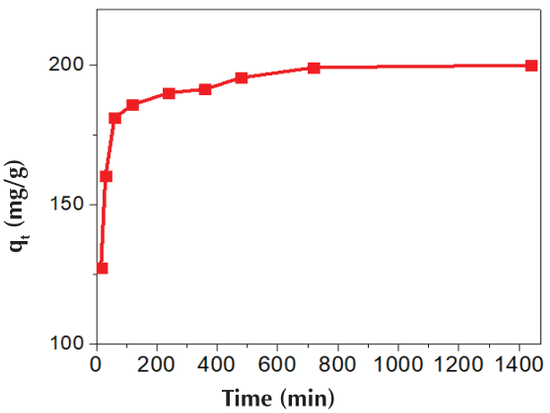

Fig. 4. Effect of contact time on the adsorption of MB on GA.

The correlation coefficient (R^2) from linear *pseudo-second-order* was closed to 1 (R^2 = 0.9999) as shown in Fig. 5. The adsorption process of MB into GA fitted well with the *pseudo-second-order* kinetic.

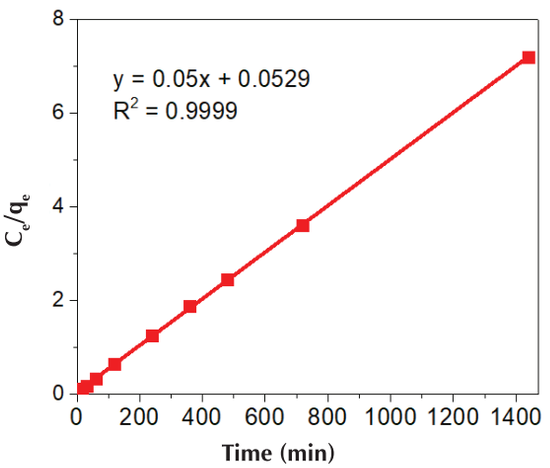

Fig. 5. The *pseudo-second-order* kinetic.

pH: Fig. 6 shows the effect of the initial pH on adsorption. The uptake capacity enhanced with the increase in pH value and reached the highest level at pH 7. The change of the capacity may be π-π stacking and electrostatic interactions between the functional groups on GA surface and MB [13, 18].

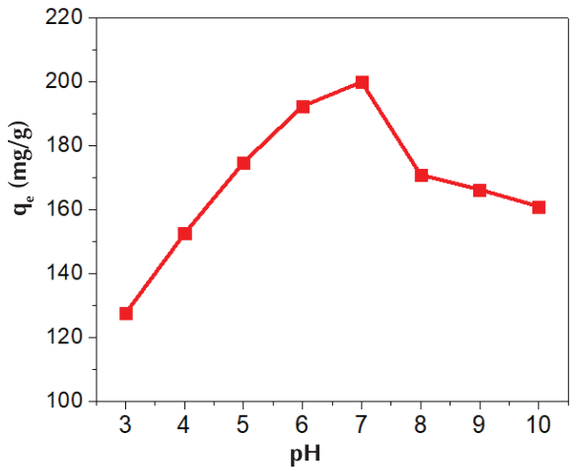

Fig. 6. Effect of pH on the adsorption of MB on GA.

Initial concentration: Fig. 7 shows the relationship between adsorption capacity and initial MB concentration. At low concentration (50-150 mg/l), the adsorption capacity was rapidly increased and at higher concentration (>150 mg/l) the adsorption capacity was slowly enhanced. This phenomenon proved that the adsorption was almost saturated.

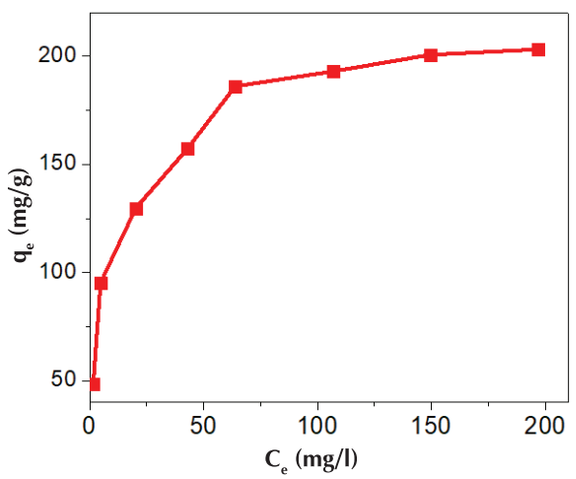

Fig. 7. Effect of initial concentration on the adsorption of MB on GA.

The correlation coefficient from Langmuir model (R^2 = 0.9979) was higher than that of Freundlich model (R^2 = 0.9408) (Fig. 8). The adsorption process for MB into GA was well-fitted to Langmuir isotherm model with the maximum adsorption capacity of 212.76 mg/g.

The maximum adsorption capacity of MB on GA compared with graphene-based materials is shown in Table 4. The results were higher compared to other materials, which indicated that the interconnected porous structure of GA increased the MB diffusion process, leading to enhancement of the adsorption capacity.

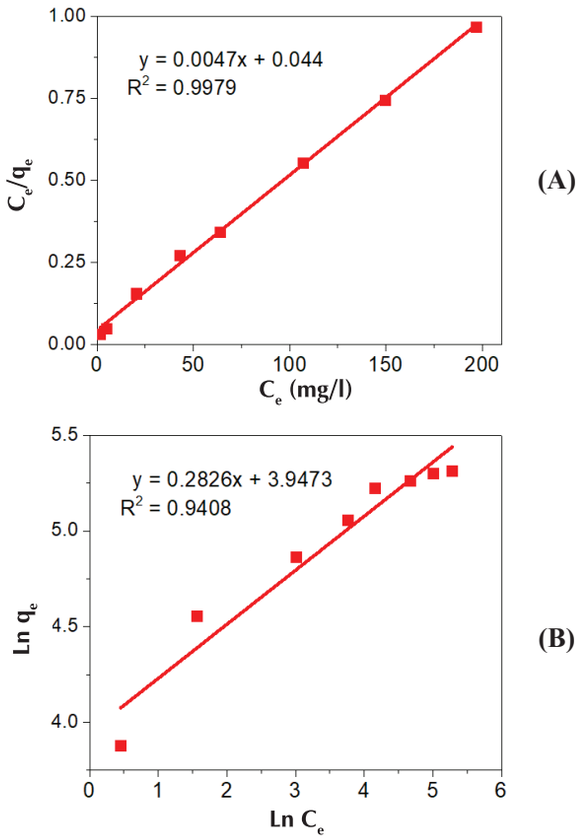

Fig. 8. Langmuir (A) and Freunlich (B) isotherm models for adsorption MB on GA.

Table 4. Maximum adsorption capacity (q_m) of various adsorbent.

Adsorbent	q_m (mg/g)	References
GA	212.76	Present work
Ge	100.0	[20]
TiO_2 (P25) - GH	87.63	[21]

Conclusions

In this study, GA was successfully synthesised by chemical reduction method. SEM images showed self-assembly of reduced GO to form porous 3D framework. FTIR, XRD and Raman results indicated that the oxygen-containing functional groups were partially reduced and GO was transformed into rGO. It was found that the suitable content of EDA for the synthesis of GA is 30 µl. GA had the maximum adsorption capacities for lubricant and crude oils, which were 160 g/g and 110 g/g respectively. The equilibrium time for adsorption of MB into the GA was 480 mins. The adsorption process of MB on GA fitted to the *pseudo-second-order* kinetic and Langmuir isotherm model with the maximum capacity of 212.76 mg/g at pH

7. Accordingly, GA could be considered as a promising adsorbent for removal of oils and MB from water.

ACKNOWLEDGEMENTS

The authors gratefully acknowledge the financial support from the Ho Chi Minh city Department of Science and Technology through the contract No. 234/2017/HD-SKHCN.

The authors declare that there is no conflict of interest regarding the publication of this article.

REFERENCES

[1] J. Huang and Z. Yan (2018), "Adsorption mechanism of oil by resilient graphene aerogels from oil-water emulsion", *Langmuir*, **34(5)**, pp.1890-1898.

[2] P.K. Malik (2004), "Dye removal from wastewater using activated carbon developed from sawdust: adsorption equilibrium and kinetics", *Journal of Hazardous Materials*, **113(1)**, pp.81-88.

[3] Y. Cheng, P. Xu, W. Zeng, C. Ling (2017), "Highly hydrophobic and ultralight graphene aerogel as high eficiency oil absorbent material", *Journal of Environmental Chemical Engineering*, **5(2)**, pp.1957-1963.

[4] T. Wu, M. Chen, L. Zhang, X. Xu, Y. Liu (2013), "Three-dimensional graphene-based aerogels prepared by a self-assembly process and its excellent catalytic and absorbing performance", *J. Mater. Chem. A*, **1**, pp.7612-7621.

[5] M.A. Worsley, T.T. Olson, J.R.I. Lee, T.M. Willey (2011), "High surface area, sp^2-cross-linked three-dimensional graphene monoliths", *J. Phys. Chem. Let.*, **8**, pp.921-925.

[6] Y. Xu, et al. (2010), "Self-assembled graphene hydrogel via a one step hydrothermal process", *ACS Nano*, **4**, pp.4324-4330.

[7] H. Sun, Z. Xu, C. Gao (2013), "Multifunctional, ultra-flweight, synergistically assembled carbon aerogels", *Adv. Mater.*, **25**, pp.2554-2560.

[8] G. Gorgolis, C. Galiotis (2017), "Graphene aerogels: a review", *2D Mater.*, **4**, p.032001.

[9] W. Chen and L. Yan (2011), "*In situ* self-assembly of mild chemical reduction graphene for three-dimensional architectures", *Nanoscale*, **3**, pp.3132-3137.

[10] K.X. Sheng, et al. (2011), "High-performance self-assembled graphene hydrogels prepared by chemical reduction of graphene oxide", *New Carbon Mater.*, **26**, pp.9-15.

[11] D.C. Marcano, D.V. Kosynkin, J.M. Berlin, A. Sinitskii, Z. Sun, A. Slesarev, Lawrence, B. Alemany, W. Lu, and J.M. Tour (2010), "Improved synthesis of graphene oxide", *ACS Nano*, **4(8)**, pp.4806-4814.

[12] C. Chi, H. Xu, K. Zhang, Y. Wang (2015), "3D hierarchical porous graphene aerogels for highly improved adsorption and recycled capacity", *Materials Science and Engineering B*, **194**, pp.62-67.

[13] P. Wang, M. Cao, C. Wang (2014), "Kinetics and thermodynamics of adsorption of methylene blue by a magnetic graphene-carbon nanotube composite", *Applied Surface Science*, **290**, pp.116-124.

[14] Yangsu Xie, Shen Xu, Zaoli Xu, Hongchao Wu, Cheng Deng (2016), "Interface-mediated extremely low thermal conductivity of graphene aerogel", *Carbon*, **98**, pp.381-390.

[15] X. Xu, H. Li, Q. Zhang, H. Hu (2015), "Self-sensing, ultralight and conductive 3D Graphene/iron oxide aerogel elastomer deformable in magnetic field", *ACS Nano*, **9(4)**, pp.3969-3977.

[16] Y.L. He, J.H. Li, J.B. Chen (2016), "The synergy reduction and self-assembly of graphene oxide via gamma-ray irradiation in an ethanediamine aqueous solution", *Nuclear Science and Techniques*, **27**, pp.61-69.

[17] J. Li, H. Meng, S. Xie, B. Zhang, L. Li (2014), "Ultra-light, compressible and fire-resistant graphene aerogel as the highly efficient and recyclable absorbent for organic liquids", *Journal of Materials Chemistry A*, **2**, pp.2934-2941.

[18] W. Si, X. Wu, J. Zhou, F. Guo, S. Zhuo (2013), "Reduced graphene oxide aerogel with high-rate supercapacitive performance in aqueous electrolytes", *Nanoscale Res. Lett.*, **8(1)**, pp.247.

[19] W. Wan, F. Zhang, S. Yu, R. Zhang (2016), "Hydrothermal formation of graphene aerogel for oil sorption: the role of reducing agent, reaction time and temperature", *New J. Chem.*, **40**, pp.3040-3046.

[20] T. Liu, Y. Li, Q. Du (2012), "Adsorption of methylene blue from aqueous solution by graphene", *Colloids and Surfaces B: Biointerfaces*, **90**, pp.197-203.

[21] C. Hou, et al. (2012), "P25-graphene hydrogels: room-temperature synthesis and application for removal of methylen blue from aqueous solution", *Journal of Hazardous Materials*, **206**, pp.229-235.